Progress In Electromagnetics Research M, Vol. 22, 149–162, 2012

DISPERSION CHARACTERISTICS AND OPTIMIZATION OF REFLECTIVITY OF BINARY ONE DIMENSIONAL PLASMA PHOTONIC CRYSTAL HAVING LINEARLY GRADED MATERIAL

S. Prasad, V. Singh*, and A. K. Singh

Department of Physics, Faculty of Science, Banaras Hindu University, Varanasi 221005, India

Abstract—The effect of graded permittivity profiles, filling factor and incident angles on the dispersion characteristics and reflectivity of binary one dimensional plasma photonic crystals having linearly graded dielectric materials are investigated by using the transfer matrix method. It is observed that position, width of band gap and high reflectance range can be improvised to desired level by proper choice of filling factor and graded permittivity index. The incident angle is found to affect the band gap and high reflectance range. Our analysis also shows that this plasma photonic crystal may be used for sensing applications.

1. INTRODUCTION

The photonic crystals or photonic band gap materials are the periodically arranged dielectric materials (or metals) which have ability to control electromagnetic waves [1, 2]. These photonic crystals have forbidden frequency regions in which the electromagnetic waves cannot propagate. These forbidden frequency regions are called photonic band gaps. The photonic crystals have gained archival interest during the past decade because of novel optical properties. These properties can be utilized in the several scientific and technical areas such as filters, optical switches, waveguides, cavities and design of more efficient layers, etc. The concept of a photonic crystal has been rapidly extended to other materials such as negative index materials, plasma, etc. Moreover, plasma has got much attention due to its technical applications in many new devices such plasma

Received 10 October 2011, Accepted 9 December 2011, Scheduled 19 December 2011

* Corresponding author: Vivek Singh (viveks@bhu.ac.in).

lens [3], plasma antenna [4], plasma stealth aircraft [5], etc. It is a well-known fact that when electromagnetic waves are launched near the plasma slab, then the electromagnetic waves with angular frequency (ω) smaller than plasma frequency (ω_p) are attenuated while those having higher frequency than plasma frequency get transmitted. But these behaviors get modified when we have spatially periodic plasma structures. These periodic structures are called plasma photonic crystals (PPCs), in which one unit cell consists of homogeneous unmagnetized (magnetized) plasma and homogeneous dielectric (vacuum). Now, electromagnetic wave whose frequency is outside the photonic band gaps even smaller than the plasma frequency can also propagate through plasma. The electromagnetic waves with frequency inside the photonic band gaps, even higher than plasma frequency, is attenuated. The concept of PPCs was proposed by Hojo and Mase [6] as a plasma version of photonic crystal in 2004. They studied the dispersion characteristics of one dimensional (1D) PPCs. Subsequently, lots of theoretical, simulated, and experimental studies have been done in one and two dimensional PPCs [7–11]. Guo [12] studied obliquely incident electromagnetic wave propagation in 1D-PPCs and concluded that plasma density, collision frequency, plasma width, dielectric constant of background materials and incident angle have marked influence on dispersion. Prasad et al. [13, 14] have investigated the modal propagation characteristics of ternary 1D-PPCs and shown that the plasma frequency, plasma width and dielectric constant of dielectric media have influence on band gap, group index, group velocity and phase velocity.

In most of the above studies, researchers have analyzed the properties of the plasma photonic crystals, which have a series of unit cells having homogeneous plasma and homogeneous dielectric layers. The effect of different parameters, such as plasma frequency, plasma density, width of plasma, dielectric constant of dielectric layer on the band gap or optical properties of PPCs by replacing homogeneous dielectric with graded dielectric materials, have not studied yet. However, the concept of functionally graded material was proposed in 1987 by Nino to develop high performance heat-resistant materials [15, 16]. Thereafter, many researchers [17–21] have investigated the change in physical properties of graded materials. These studies show that the change of physical properties of graded materials has very different behaviors from the homogeneous materials and conventional composite materials. Sang nd Li [20] have studied the optical properties of one dimensional photonic crystal containing graded materials and found that the gradation profiles of permittivity have marked influences on band gaps. They also studied the properties of defect modes in one-dimensional photonic crystals containing a graded defect layer [21] and found that the introduction of a graded defect layer in one dimensional photonic crystal provides possible mechanism for tuning the defect modes including the position, intensity, and number of modes. Recently, some research groups [22, 23] have analyzed the property of 1D-PPCs by replacing homogeneous dielectric layer with exponentially graded layer and found very interesting and novel results.

It is clear from above discussion that the propagation characteristics of photonic crystals can also be controlled by the gradation profile of graded materials. Therefore, in the present analysis, a linearly graded material in the unit cell of PPCs in place of homogeneous dielectric layer is chosen for the first time in our knowledge. The objective is to get extra degrees of freedom to control the dispersion characteristics and reflectivity preserving the plasma behavior of photonic crystal. Also, this linearly graded material can easily be solved in term of well defined standard special functions, such as Airy function and Bessel function. The organization of the paper is as follows. In Section 2, the dispersion relation and reflectivity of the proposed structure is given. The other necessary formulas used in this paper are also presented. Section 3 is devoted to result and discussion. A conclusion is drawn in section 4.

2. THEORETICAL FORMULATION

The structure having plasma and linearly graded dielectric material in one unit cell is shown in Fig. 1. The plane electromagnetic waves are injected obliquely onto the binary one dimensional plasma photonic crystals from the vacuum at a certain angle θ_0. The plasma layer is characterized by frequency dependent permittivity (ε_p), and the graded dielectric layer is characterized by linear spatial dependent permittivity profile (ε_g). The linear variation in permittivity profile index is taken in z-direction which is normal to the interface. The TE mode of electric field is considered in x-y plane. The collisions in the plasma layer and absorption in the linearly graded materials are neglected. It is assumed that plasma and graded dielectric materials are non-magnetic in nature. The permittivity profiles are given below:

$$\varepsilon(\omega, z) = \begin{cases} \varepsilon_p = 1 - \dfrac{\omega_p^2}{\omega^2}; & n\Lambda - a < z < n\Lambda \\ \varepsilon_g = lz + m; & (n-1)\Lambda < z < n\Lambda - a \end{cases} \quad (1)$$

with condition that $\varepsilon(\omega, z) = \varepsilon(\omega, z + \Lambda)$, where $\omega_p = \sqrt{e^2 n_p / \varepsilon_0 m_e}$ is the plasma frequency, m_e the rest mass of electron, n_p the density of

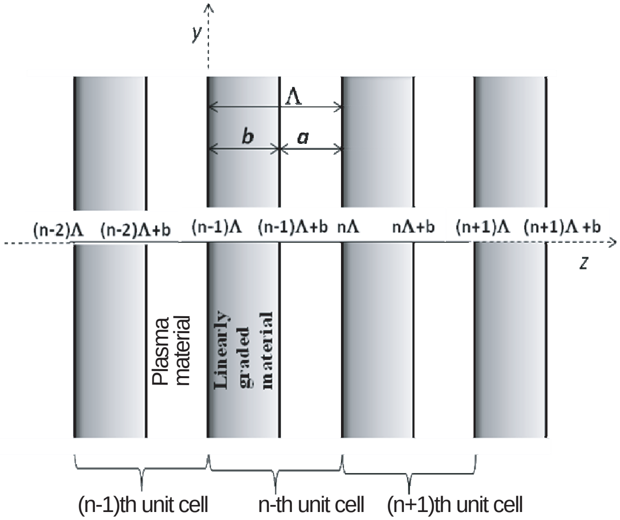

Figure 1. Schematic representation of the unit cell of 1-D BPPC having linearly graded material.

plasma, m the permittivity at $z = 0$, l the linear gradation parameter for controlling permittivity in the graded layer ($l = \frac{1}{b}(\varepsilon_g - m)$), $\Lambda = a + b$, and a and b the width of plasma layer and graded layer, respectively. The wave equation for the electric field is

$$\frac{\partial^2 E_x(y,z)}{\partial y^2} + \frac{\partial^2 E_x(y,z)}{\partial z^2} + \frac{\omega^2}{c^2}\varepsilon(\omega,z)E_x(y,z) = 0 \tag{2}$$

Since the variation of permittivity is only in z-direction, the wave-vector k_y is conserved. By using Snell's law of refraction, it can be written as $k_y = \frac{\omega}{c}n_g \sin(\theta) = \frac{\omega}{c}n_0 \sin(\theta_0)$, where n_g and n_0 are the refractive indices of the graded layer and vacuum respectively and given as: $n_g = \sqrt{\varepsilon_g}$, $n_0 = \sqrt{\varepsilon_0}$.

The wave equation for both layers in the nth unit cell can be written separately as:

$$\frac{d^2E(z)}{dz^2} + \frac{\omega^2}{c^2}\left(1 - \frac{\omega_p^2}{\omega^2} - \sin^2\theta_0\right)E(z) = 0; \quad n\Lambda - a < z < n\Lambda \tag{3}$$

$$\frac{d^2E(z)}{dz^2} + \frac{\omega^2}{c^2}\left(lz + m - \sin^2\theta_0\right)E(z) = 0; \quad (n-1)\Lambda < z < n\Lambda - a \tag{4}$$

Solutions for electric field in both regions in nth unit cell for

$\omega > \omega_{pe}$ are given:

$$E(z) = \begin{cases} a_n e^{ik_p(z-n\Lambda)} + b_n e^{-ik_p(z-n\Lambda)}; & n\Lambda - a < z < n\Lambda \\ c_n Ai(-zi1) + d_n Bi(-zi1); & (n-1)\Lambda < z < n\Lambda - a \end{cases} \quad (5)$$

where $k_p = \frac{\omega}{c}\sqrt{1 - \frac{\omega_p^2}{\omega^2} - \sin^2(\theta_0)}$, $zi1 = (\frac{\omega^2}{c^2} l)^{1/3}(z - n\Lambda + a + \frac{1}{l}(m - \sin^2(\theta_0)))$, Ai and Bi are well documented Airy functions [24]. When $\omega < \omega_p$, k_p in above equation becomes imaginary, thus, electromagnetic waves will not propagate in the plasma medium. Hence the above solution for $\omega < \omega_p$ is written as:

$$E(z) = \begin{cases} a_n e^{\kappa(z-n\Lambda)} + b_n e^{-\kappa(z-n\Lambda)} & n\Lambda - a < z < n\Lambda \\ c_n Ai(-zi1) + d_n Bi(-zi1); & (n-1)\Lambda < z < n\Lambda - a \end{cases} \quad (6)$$

where $\kappa = \frac{\omega}{c}\sqrt{\frac{\omega_p^2}{\omega^2} - 1 - \sin^2(\theta_0)}$. Since we are interested only in propagating waves in plasma medium therefore, we consider $\omega > \omega_p$. By making use of continuity condition of electric field $E(z)$ and its derivatives at the interfaces and using transfer matrix method [25], the following matrix relation is obtained:

$$\begin{pmatrix} a_{n-1} \\ b_{n-1} \end{pmatrix} = \begin{pmatrix} m_{11} & m_{12} \\ m_{21} & m_{22} \end{pmatrix} \begin{pmatrix} a_n \\ b_n \end{pmatrix} \quad (7)$$

The unit translation matrix elements m_{11}, m_{12}, m_{21} and m_{22} for $\omega > \omega_{pe}$ are given below:

$$\begin{aligned} m_{11} = & \frac{1}{2}\exp\big(Ai(-zi2)Bi'(-zi3)t_1 - Ai(-zi2)Bi(-zi3) \\ & + t_1^2 Ai'(-zi2)Bi'(-zi3) - t_1 Ai'(-zi2)Bi(-zi3)t_1 \\ & - Bi(-zi2)Ai'(-zi3)t_1 + Bi(-zi2)Ai(-zi3) \\ & - t_1^2 Bi'(-zi2)Ai'(-zi3) + t_1 Bi'(-zi2)Ai(-zi3)t_1\big) \\ & /\big(\big(Ai(-zi2)Bi'(-zi3) - Bi(-zi2)Ai'(-zi3)\big)\, t_1\big) \end{aligned} \quad (7a)$$

$$\begin{aligned} m_{12} = & \frac{1}{2}\exp(ik_p a)\big(Ai(-zi2)Bi'(-zi3)t_1 + Ai(-zi2)Bi(-zi3) \\ & + t_1^2 Ai'(-zi2)Bi'(-zi3) + t_1 Ai'(-zi2)Bi(-zi3) \\ & - Bi(-zi2)Ai'(-zi3)t_1 - Bi(-zi2)Ai(-zi3) \\ & - t_1^2 Bi'(-zi2)Ai'(-zi3) - t_1 Bi'(-zi2)Ai(-zi3)\big) \\ & /\big((Ai(-zi3)Bi'(-zi3) - Bi(-zi3)Ai'(-zi3))t_1\big) \end{aligned} \quad (7b)$$

$$\begin{aligned} m_{21} &= \frac{1}{2}\exp(-ik_pa)\big(Ai(-zi2)Bi'(-zi3)t_1 - Ai(-zi2)Bi(-zi3) \\ &\quad -t_1^2Ai'(-zi2)Bi'(-zi3) + t_1Ai'(-zi2)Bi(-zi3) \\ &\quad -Bi(-zi2)Ai'(-zi3)t_1 + Bi(-zi2)Ai(-zi3) \\ &\quad +t_1^2Bi'(-zi2)Ai'(-zi3) - t_1Bi'(-zi2)Ai(-zi3)\big) \\ &\quad /\big((Ai(-zi3)Bi'(-zi3) - Bi(-zi3)Ai'(-zi3))t_1\big) \end{aligned} \tag{7c}$$

$$\begin{aligned} m_{22} &= \frac{1}{2}\exp(ik_pa)\big(-Ai(-zi2)Bi'(-zi3)t_1 - Ai(-zi2)Bi(-zi3) \\ &\quad +t_1^2Ai'(-zi2)Bi'(-zi3) + t_1Ai'(-zi2)Bi(-zi3) \\ &\quad +Bi(-zi2)Ai'(-zi3)t_1 + Bi(-zi2)Ai(-zi3) \\ &\quad -t_1^2Bi'(-zi2)Ai'(-zi3) - t_1Bi'(-zi2)Ai(-zi3)\big) \\ &\quad /\big((Ai(-zi3)Bi'(-zi3) - Bi(-zi3)Ai'(-zi3))t_1\big) \end{aligned} \tag{7d}$$

where $t_1 = (\frac{\omega^2}{c^2}l)^{1/3}\frac{1}{ik_p}$, $zi2 = (\frac{\omega}{cl})^{2/3}(m - \sin^2(\theta_0) - lb)$, $zi3 = (\frac{\omega}{cl})^{2/3}(m - \sin^2(\theta_0))$, Ai, Bi, Ai', Bi' are Airy functions and its derivatives. According to Floquet theorem, wave propagating in a periodic medium is of form $E_k(y,z) = E_k(z)e^{ik_zz}e^{ik_yy}$, here $E_k(z)$ is periodic with period Λ, namely, $E_k(z+\Lambda) = E_k(z)$. The dispersion relation [25] for the proposed structure can be written as:

$$K = \left(\frac{1}{\Lambda}\right)\cos^{-1}\left[\frac{1}{2}(m_{11}+m_{22})\right] \tag{8}$$

Here K is Bloch wave number. Suppose there are N unit cells in the proposed structure, then we can write Equation (7) as:

$$\begin{pmatrix} a_0 \\ b_0 \end{pmatrix} = \begin{pmatrix} m_{11} & m_{12} \\ m_{21} & m_{22} \end{pmatrix}^N \begin{pmatrix} a_n \\ b_n \end{pmatrix} \tag{9}$$

Now, the coefficient of reflection of the structure can be derived by using the relation:

$$r_N = \left({b_0}/{a_0}\right)_{b_n=0} \tag{10}$$

Here a_0 and b_0 represent the complex amplitudes of incident and reflected waves, and the condition $b_n = 0$ implies the boundary condition that to the right of the periodic structure, there is no wave incident on the structure.

Simplifying this equation, the coefficient of reflection can be expressed as:

$$r_N = \left(\frac{CU_{N-1}}{AU_{N-1} - U_{N-2}}\right) \tag{11}$$

where $U_N = \sin(N+1)K\Lambda/\sin K\Lambda$.

Hence, the reflectivity of the proposed structure can be expressed as

$$Rf = |r_N|^2 = \frac{|C|^2}{|C|^2 + (\sin K\Lambda/\sin(N+1)K\Lambda)^2} \tag{12}$$

3. RESULT AND DISCUSSIONS:

The effect of filling factor, permittivity profile index of the graded dielectric layer and incident angles on the band gaps and reflectivity are analyzed by using Equations (8) and (12). The unit cell of the proposed structure consists of the plasma layer having thickness a and graded dielectric layer with width b ($b = f \times a$, for $f = 1$, $a = b$). The parameters which are used in numerical calculations are: a, f (filling factor, $f = b/\Lambda$), θ_0 (angle of incident), p (normalized plasma frequency, $p = \omega_p c/a$), normalized frequency ($\omega c/a$), total number of unit cells N and the permittivity ε_b at $x = b$. Here m (the value of permittivity at $x = 0$) is designated by ε_0. For $p = 0.2$, the plasma frequency ω_p is 1.2×10^{11} /sec. In all the numerical calculations, different permittivity profile indices are taken in such a way that average volume permittivity remains fixed at 3.5.

Figure 2 shows the effect of filling factor on the band gap for $a = 500\,\mu\text{m}$, $\theta_0 = 0$, $p = 0.2$, $\varepsilon_b = 4.0$ and $\varepsilon_0 = 3.0$. It is observed that for $f = 0.5$, there is no band gap obtained in the considered frequency range. The first band gap for $f = 0.5$ is obtained at the normalized frequency 13.38 which is not shown in the figure. As the filling factor increases from 0.5 to 1.5, band structure formation takes place in considered normalized frequency range and position of band gap shifted towards lower frequency range. For $f = 1.0$, the first band gap is at normalized frequency ~ 4.65, and for $f = 1.5$, it is approximately at 1.8. Hence the width of band gap decreases, and number of band gaps is increased with an increase in the filling factor. It is also observed that the phase velocity highly depends on the filling factor and becomes slower with an increase of filling factor. These results can be explained as: a number of continuous interfaces can be considered to exist in the graded layers profile which leads to modifying the reflection due to these interfaces. Fig. 3 shows the effect of graded permittivity profiles on the band gap for $a = 500\,\mu\text{m}$, $f = 1.0$, $\theta_0 = 0$ and $p = 0.2$. Here the graded permittivity profiles $\varepsilon_b = 6.0$, $\varepsilon_0 = 1.0$ (solid lines) and $\varepsilon_b = 4.0$, $\varepsilon_0 = 3.0$ (dotted lines) are taken in such a way that average volume permittivity remains fixed at 3.5. A comparison is made by replacing graded dielectric material with a homogeneous dielectric material having constant permittivity

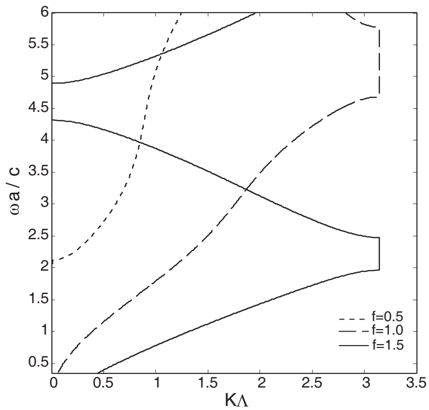

Figure 2. The band gap for $a = 500\,\mu\mathrm{m}$, $\theta_0 = 0$, $p = 0.2$, $\varepsilon_b = 4.0$ and $\varepsilon_0 = 3.0$ for different values of f.

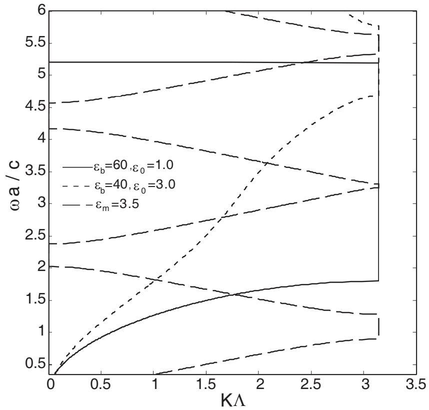

Figure 3. The band gap for $a = 500\,\mu\mathrm{m}$, $f = 1.0$, $\theta_0 = 0$ and $p = 0.2$ for different permittivity profiles index.

3.5 (dash line). It is found that for $\varepsilon_b = 6.0$, $\varepsilon_0 = 1.0$ (solid line), the width of first band gap is much wider than those for $\varepsilon_b = 4.0$, $\varepsilon_0 = 3.0$ (dotted line), and the position of band gap is different. This implies that by choosing a suitable graded permittivity profile, we can tune the width as well as the position of band gap at any desired level, which is a novelty of the present study. By comparing these different graded permittivity profiles with a homogeneous dielectric $\varepsilon_m = 3.5$ (dash line), it is observed that band gap width and phase velocities are larger in the graded profiles. Fig. 4 shows the effect of incident angle on the band gap for $a = 500\,\mu\mathrm{m}$, $f = 1.0$, $\theta_0 = 0$, $p = 0.2$, $\varepsilon_b = 4.0$ and $\varepsilon_0 = 3.0$. It is found that with an increase in the incident angle θ_0 from 0 to $\pi/3$, the band gaps shift towards lower frequencies range, and the width of band gap is increased. Hence, it can be concluded that incident angle also affects the position, width of the band gap and phase velocity.

Moreover, the High Reflectance Range (HRR), where $Rf \approx 1$, is optimized by changing the filling factor and graded permittivity profiles. The effect of incident angle on HRR is also investigated. The variation of the reflectivity for $a = 500\,\mu\mathrm{m}$, $\theta_0 = 0$, $p = 0.2$, $N = 3$, $\varepsilon_b = 6.0$ and $\varepsilon_0 = 1.0$ at different values of filling factor is shown in Fig. 5. It is observed that HRR is maximum when $f = 1.5$ in the frequency range 1.75–3.0. Fig. 6 shows the variation of reflectivity for $a = 500\,\mu\mathrm{m}$, $f = 1.5$, $\theta_0 = 0$, $N = 3$ and $p = 0.2$ for different graded permittivity profiles keeping volume average permittivity constant at

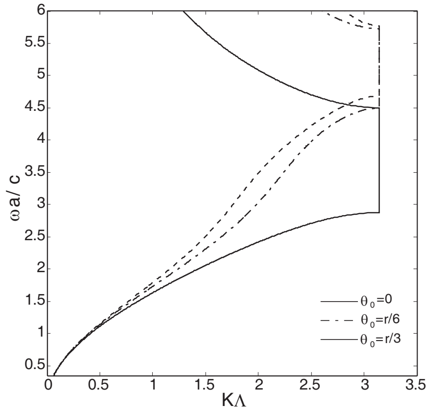

Figure 4. The band gap for $a = 500\,\mu\text{m}$, $f = 1.0$, $\theta_0 = 0$, $p = 0.2$, $\varepsilon_b = 4.0$ and $\varepsilon_0 = 3.0$ for different incident angle.

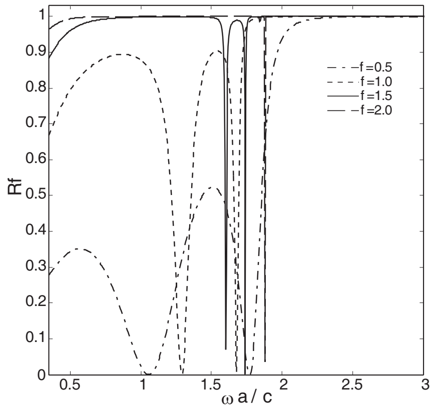

Figure 5. The reflectivity for $a = 500\,\mu\text{m}$, $\theta_0 = 0$, $p = 0.2$, $N = 3$, $\varepsilon_b = 6.0$ and $\varepsilon_0 = 1.0$ at different values of f.

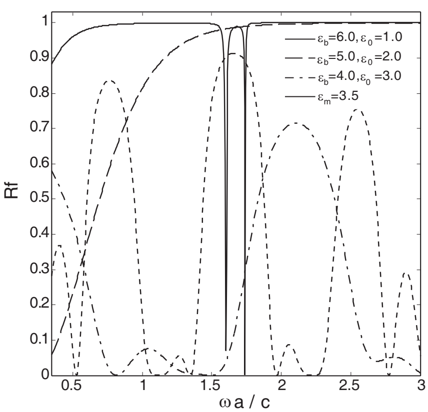

Figure 6. The reflectivity for $a = 500\,\mu\text{m}$, $f = 1.5$, $\theta_0 = 0$, $N = 3$ and $p = 0.2$ for different permittivity profiles index.

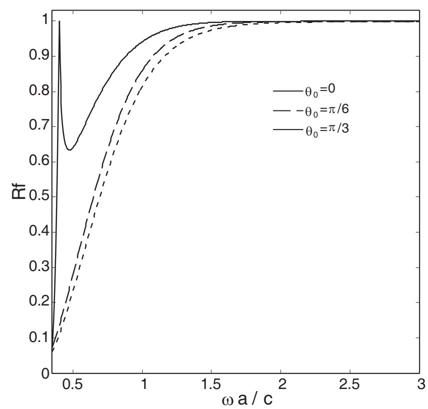

Figure 7. The reflectivity for $a = 500\,\mu\text{m}$, $f = 1.5$, $\theta_0 = 0$, $p = 0.2$, $N = 3$, $\varepsilon_b = 5.0$ and $\varepsilon_0 = 2.0$ for different angle of incidence.

3.5. It is found that HRR is maximum for $\varepsilon_b = 6.0$ and $\varepsilon_0 = 1.0$, which is consistent with band gap analysis (Fig. 3). It is observed that HRR can be tune by taking different graded permittivity profiles. For the comparison purpose, we have also plotted the reflectivity by replacing graded dielectric layer with a homogeneous dielectric layer having permittivity constant $\varepsilon_m = 3.5$ (dotted line). In this case no

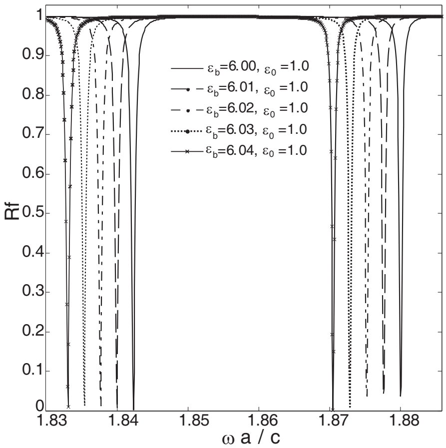

Figure 8. The shift of dip of reflectivity for $a = 500\,\mu\text{m}$, $f = 2.0$, $\theta_0 = 0$, $p = 0.2$, $N = 3$ and $\varepsilon_0 = 1.0$ at different values of ε_b.

HRR is found in the considered frequency range. From the above analysis of reflectivity (Figs. 5 and 6), it can be concluded that HRR is maximum when $a = 500\,\mu\text{m}$, $f = 1.5$, $\theta_0 = 0$, $p = 0.2$, $\varepsilon_b = 6.0$ and $\varepsilon_0 = 1.0$, due to the fact that the sharp varying permittivity of graded dielectric layer increases the Bragg's reflection. The effect of incident angle on the reflectivity for $a = 500\,\mu\text{m}$, $f = 1.5$, $\theta_0 = 0$, $p = 0.2$, $N = 3$, $\varepsilon_b = 5.0$ and $\varepsilon_0 = 2.0$ is shown in Fig. 7. It is observed that when incident angle increases from 0 to $\pi/3$, HRR is enhanced. The shift of dip in the reflectivity for $a = 500\,\mu\text{m}$, $f = 2.0$, $\theta_0 = 0$, $p = 0.2$, $N = 3$ and $\varepsilon_0 = 1.0$ by varying ε_b is also studied, which is shown in Fig. 8. Here graded profile $\varepsilon_0 = 1.0$ and $\varepsilon_b = 6.0$ is taken because it shows the sharp reflection dips. It is observed that for a small increment (0.01) in the ε_b, these dips of reflectivity are shifted towards lower frequency. This shift of position of reflection dips is the sensor signal and may be utilized for sensing purpose, where the slope of the curve will give the sensitivity while the shift of dip gives the concentration/amount which causes to change in dielectric permittivity.

However, to understand the propagation of wave in the proposed structures we plot the electric field distribution. The upper half of Fig. 9 shows the electric field distribution in one unit cell having graded profile of permittivity and plasma while the lower half of Fig. 9 shows the electric field distribution in one unit cell having constant permittivity and plasma. Here both unit cells considered in Fig. 9 possess the same volume-average permittivity (3.5). It is observed that

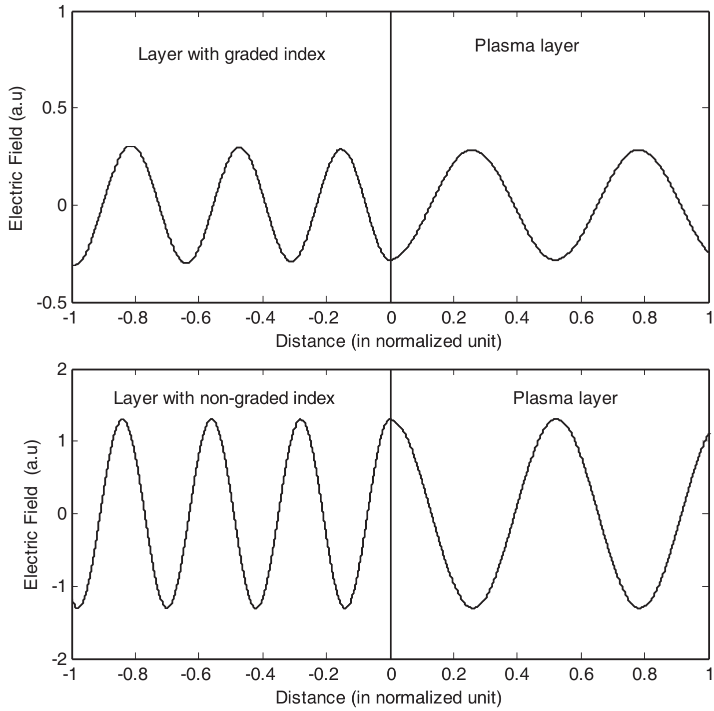

Figure 9. The electric field distribution of proposed PPC structures having same volume average permittivity.

the electric field distribution obtained in graded profile is different from the non-graded profile, although the volume average permittivity is the same. The amplitude of electric field is continuously decreasing with increasing propagation depth in the graded profile. The decrease of amplitude occurs due to the presence of inhomogeneity in graded layer which may be explained by considering many continuous interfaces within the graded layers.

4. CONCLUSIONS

The dispersion characteristics and reflection spectra of binary one dimensional plasma photonic having linearly graded materials are being investigated in the present study. The equations for dispersion relation and reflectivity are derived by solving Maxwell equations employing the continuity conditions of electric fields and its derivative using transfer matrix method. It is found that the position and width of the band gap can be improvised by filling factor and the proper choice of graded permittivity profiles keeping average volume permittivity constant. Also, it is observed that the angle of incidence affects the band gap. By the analysis of reflection spectra, high reflectance range ($Rf \approx 1$) is found to be tuned by filling factor, varying graded permittivity profile and incident angle. It is observed that high reflectance range is optimized to maximum for $a = 500\,\mu\text{m}$, $f = 1.5$, $\theta_0 = 0$, $p = 0.2$, $\varepsilon_b = 6.0$ and $\varepsilon_0 = 1.0$, and with increase in incident angle, high reflectance range is enhanced. Also, the sharp reflection dips obtained in the present analysis may be utilized for sensing or other applications.

ACKNOWLEDGMENT

The authors are grateful to Dr. B. Prasad and Dr. R. D. S. Yadava for their continuous encouragement and supports in many ways.

REFERENCES

1. Yablonovitch, E., "Inhibited spontaneous emission in solid-state physics and electronics," *Phys. Rev. Lett.*, Vol. 58, 2059–2063, 1987.
2. John, S., "Strong localization of photons in certain disordered dielectric superlattice," *Phys. Rev. Lett.*, Vol. 58, 2486–2489, 1987.
3. Goncharov, A. A., A. V. Zatuagan, and I. M. Protsenko, "Focusing and control of multiaperture ion beams by plasma lenses," *IEEE Trans. on Plasma Sci.*, Vol. 21, No. 5, 578–581, 1993.
4. Dwyer, J. G., D. Murphy, J. Perin, R. Pechacek, and M. Raleigh, "On the feasibility of using an atmospheric discharge plasma as an RF antenna," *IEEE Trans. on Antennas and Propag.*, Vol. 32, No. 2, 141–146, 1984.
5. Vidmar, R. J., "On the use of atmospheric pressure plasmas as electromagnetic reflectors and absorbers," *IEEE Trans. on Plasma Sci.*, Vol. 18, No. 4, 733–741, 1990.
6. Hojo, H. and A. Mase, "Dispersion relation of electromagnetic waves in one-dimensional plasma photonic crystals," *J. Plasma Fusion Res.*, Vol. 80, 89–90, 2004.
7. Shiveshwari, L. and P. Mahto, "Photonic band gap effect in one-dimensional plasma dielectric photonic crystals," *Solid State Commun.*, Vol. 138, 160–164, 2006.
8. Sakai, O., T. Sakaguchi, and K. Tachibana, "Verification of a plasma photonic crystal for microwaves of millimeter wavelength

range using two-dimensional array of columnar microplasmas," *Appl. Phys. Lett.*, Vol. 87, 241505-241505-3, 2005.

9. Song, L., Z. Shuangying, and L. Sanqiu, "A study of properties of the photonic band gap of unmagnetized plasma photonic crystal," *Plasma Science and Technology*, Vol. 11, No. 1, 14–17, 2009.
10. Qi, L. and Z. Yang, "Modified plane wave method analysis of dielectric plasma photonic crystal," *Progress In Electromagnetics Research*, Vol. 91, 319–332, 2009.
11. Qi, L., Z. Yang, F. Lan, X. Gao, and Z. Shi, "Properties of obliquely incident electromagnetic wave in one-dimensional magnetized plasma photonic crystals," *Physics of Plasmas*, Vol. 17, 042501-042501-8, 2010.
12. Guo, B., "Photonic band gap structures of obliquely incident electromagnetic wave propagation in a one-dimension absorptive plasma photonic crystal," *Physics of Plasmas*, Vol. 16, 043508-043508-6, 2009.
13. Prasad, S., V. Singh, and A. K. Singh, "Modal propagation characteristics of EM waves in ternary one-dimensional plasma photonic crystals," *Optik, International Journal for Light and Electron Optics*, Vol. 121, No. 16, 1520–1528, 2010.
14. Prasad, S., V. Singh, and A. K. Singh, "A comparative study of dispersion relation of EM waves in ternary one-dimensional plasma photonic crystals having two different structures," *Optik, International Journal for Light and Electron Optics*, Vol. 122, 1279–1283, 2011.
15. Nino, M., T. Hirai, and R. Watanabe, "The functionally gradient materials," *J. Jpn. Soc. Compos. Mater.*, Vol. 13, 257–260, 1987.
16. Suresh, S. and A. Mortensen, "Fundamentals of functionally graded materials," *IOM Communications Ltd.*, The Institute of Materials, London, 1998.
17. Hui, P. M., X. Zhang, A. J. Markworth, and D. Stroud, "Thermal conductivity of graded composites: Numerical simulations and an effective medium approximation," *J. Mater. Science*, Vol. 34, 5497–5503, 1999.
18. Huang, J. P. and K. W. Yu, "Effective nonlinear optical properties of graded metal-dielectric composite films of anisotropic particles," *J. Opt. Soc. Am. B*, Vol. 22, 1640–1647, 2005.
19. Gao, L., J. P. Huang, and K. W. Yu, "Effective nonlinear optical properties of composite media of graded spherical particles," *Phys. Rev. B*, Vol. 69, 075105–075113, 2004.
20. Sang, Z. F. and Z. Y. Li, "Optical properties of one-

dimensional photonic crystals containing graded materials," *Optics Communications*, Vol. 259, 174–178, 2006.

21. Sang, Z. F. and Z. Y. Li, "Properties of defect modes in one-dimensional photonic crystals containing a graded defect layer," *Optics Communications*, Vol. 273, 162–166, 2007.
22. Prasad, S., V. Singh, and A. K. Singh, "Modeling of a filter from one-dimensional plasma photonic crystal having exponentially graded material in submillimeter range," *Journal of Optics Research*, Vol. 12, Nos. 3–4, Article 2, 2011.
23. Prasad, S., V. Singh, and A. K. Singh, "Effect of inhomogeneous plasma density on the reflectivity in one dimensional plasma photonic crystal," *Progress In Electromagnetics Research M*, Vol. 21, 211–222, 2011.
24. Abramowitz, M. and I. A. Stegun, *Handbook of Mathematical Functions*, Applied Mathematics Series, 55, National Bureau of Standard, 1964.
25. Yeh, P., *Optical Waves in Layered Media*, 2nd edition, Wiley-Interscience, 2005.